International Journal of Current Engineering and Technology
ISSN 2277 - 4106
© 2013 INPRESSCO. All Rights Reserved.
Available at http://inpressco.com/category/ijcet

Research Article

Elaboration and Characterization of Bioceramic Based on Tricalcium Phosphate and Zirconia

Imen Sallemi[Å], Jamel Bouaziz[Å] and Foued Ben Ayed[Å*]

[Å]Laboratory of Industrial Chemistry, National School of Engineering, Box 1173, 3038, Sfax University ,Sfax, Tunisia

Accepted 01 November 2013, Available online 01 December 2013, **Vol.3, No.5 (December 2013)**

Abstract

The effect of the sintering temperature on the mechanical properties of the tricalcium phosphate – zirconia composites were investigated between 1300°C and 1600°C and with different quantities of tricalcium phosphate (25 wt%, 50 wt% and 75 wt%). The characteristics of the samples after and before the sintering process were realized by differential thermal analysis, dilatometry, X-ray diffraction, ^{31}P magic angle scanning nuclear magnetic resonance, scanning electron microscope and mechanical testing with the Brazilian test. The mechanical strength of the tricalcium phosphate – zirconia composites increased with the sintering temperature. At 1600°C, the mechanical properties of the tricalcium phosphate – 75 wt% zirconia composites achieved their maximum value. The addition of tricalcium phosphate stabilized the structure of zirconia and partially prevented the inverse allotropic transformation from the tetragonal phase to the monoclinic phase.

Keywords*: Sintering process, Mechanical properties, Composites, Microstructure, Tricalcium phosphate, Zirconia, Bioceramic.*

1. Introduction

Bioceramics have been sought as biomaterials for reconstruction of bone defect in maxillofacial, dental and orthopedic applications (P. Ducheyne *et al*, 1981; C. Lavernia *et al*, 1991; L.L. Hench, 1991; L.L. Hench, 1993; J. Li *et al*, 1993; Y.J. Horng *et al*, 1994; JC. Elliott, 1994; L.L. Hench, 1998; I. Levin *et al*, 1998; E. Landi *et al*, 2000; F. Ben Ayed *et al*, 2000; F. Ben Ayed *et al*, 2001; H. K. Varma *et al*, 2001 ; R. Rao. Ramachandra *et al*, 2002 ; H.S. Ryu *et al*, 2002; Yashima *et al*, 2003; A. Destainville *et al*, 2003 ; C.X. Wang *et al*, 2004; S. Hoell *et al*, 2005; R.D. Gaasbeek *et al*, 2005; S.S. Jensen *et al*, 2006; J. Chevalier, 2006; F. Ben Ayed *et al*, 2006; M. Gutierres *et al*, 2007; G.L. DeSilva *et al*, 2007; K. Lin *et al*, 2007; F. Ben Ayed *et al*, 2007; F. Ben Ayed *et al*, 2008; P. Miranda *et al*, 2008; N. Bouslama *et al*, 2009; J. Chevalier *et al*, 2009 ; K. Chaari *et al*, 2009; A.K. Guha *et al*, 2009; F.H. Perera *et al*, 2010; N. Bouslama *et al*, 2010; F. Ben Ayed, 2011; A. Guidera *et al*, 2011; S. Sakka *et al*, 2012; I. Sellami *et al*, 2012). In generally, bioceramics such as bioinert (e.g., alumina (Al_2O_3) and zirconia (ZrO_2)), resorbable (e.g., tricalcium phosphate (TCP)), and bioactive (e.g., hydroxyapatite (HAp) and fluorapatite (FAp)) are used for biomedical applications (P. Ducheyne *et al*, 1981; C. Lavernia *et al*, 1991; L.L. Hench, 1991; L.L. Hench, 1993; J. Li *et al*, 1993; Y.J. Horng *et al*, 1994; JC. Elliott, 1994; L.L. Hench, 1998; I. Levin *et al*, 1998; E. Landi *et al*, 2000; F. Ben Ayed *et al*, 2000; F. Ben Ayed *et al*, 2001; H. K. Varma *et al*, 2001 ; R. Rao. Ramachandra *et al*, 2002 ; H.S. Ryu *et al*, 2002; Yashima *et al*, 2003; A. Destainville *et al*, 2003 ; C.X. Wang *et al*, 2004; S. Hoell *et al*, 2005; R.D. Gaasbeek *et al*, 2005; S.S. Jensen *et al*, 2006; J. Chevalier, 2006; F. Ben Ayed *et al*, 2006; M. Gutierres *et al*, 2007; G.L. DeSilva *et al*, 2007; K. Lin *et al*, 2007; F. Ben Ayed *et al*, 2007; F. Ben Ayed *et al*, 2008; P. Miranda *et al*, 2008; N. Bouslama *et al*, 2009; J. Chevalier *et al*, 2009 ; K. Chaari *et al*, 2009; A.K. Guha *et al*, 2009; F.H. Perera *et al*, 2010; N. Bouslama *et al*, 2010; F. Ben Ayed, 2011; A. Guidera *et al*, 2011; S. Sakka *et al*, 2012; I. Sellami *et al*, 2012). The production of biocompatible scaffolds is a challenge for biomaterials technology. Tricalcium phosphate (β-TCP, $Ca_3(PO_4)_2$) has been known as a valuable implant material for many years (F. Ben Ayed *et al*, 2001; H. K. Varma *et al*, 2001 ; R. Rao. Ramachandra *et al*, 2002 ; H.S. Ryu *et al*, 2002; Yashima *et al*, 2003; A. Destainville *et al*, 2003 ; C.X. Wang *et al*, 2004; S. Hoell *et al*, 2005; R.D. Gaasbeek *et al*, 2005; S.S. Jensen *et al*, 2006; J. Chevalier, 2006; F. Ben Ayed *et al*, 2006); (A.K. Guha *et al*, 2009; F.H. Perera *et al*, 2010; N. Bouslama *et al*, 2010; F. Ben Ayed, 2011; A. Guidera *et al*, 2011; S. Sakka *et al*, 2012; I. Sellami *et al*, 2012; I. Levin *et al*, 1998). Indeed, the tricalcium phosphate has a good potential to be used to

* Corresponding author: **Prof. Foued BEN AYED**. Phone: 00 216 98 252 033, Fax: 00 216 74 275 595.

repair bone defects, owing to its excellent biocompatibility in the human body and to its chemical composition which is similar to the organic constituent of bone mineral (F. Ben Ayed *et al*, 2001; H. K. Varma *et al*, 2001 ; R. Rao. Ramachandra *et al*, 2002 ; H.S. Ryu *et al*, 2002; Yashima *et al*, 2003; A. Destainville *et al*, 2003 ; C.X. Wang *et al*, 2004; S. Hoell *et al*, 2005; R.D. Gaasbeek *et al*, 2005; S.S. Jensen *et al*, 2006; J. Chevalier, 2006; F. Ben Ayed *et al*, 2006). Inert ceramics oxides, like zirconia have high tribological properties (E.C. Subbarao *et al*, 1981; P. Christel *et al*, 1989; D.S. Metsger *et al*, 1999; K. Prabakaran *et al*, 2005; E. Zafer, 2007; S. Arnaud *et al*, 2011). Zirconia has attracted major attention because of the possibility of obtaining a nanograined bulk ceramic with a controllable microstructure and improved mechanical properties (E.C. Subbarao *et al*, 1981; P. Christel *et al*, 1989; D.S. Metsger *et al*, 1999; K. Prabakaran *et al*, 2005; E. Zafer, 2007; S. Arnaud *et al*, 2011). Zirconia can be mixed with tricalcium phosphate to make bioceramics composites, which would combine the biocompatibility of tricalcium phosphate and the high tribological properties of zirconia. The aim of this study is then to elaborate and sinter the tricalcium phosphate – zirconia composites at various temperatures (1300°C, 1400°C, 1500°C, 1550°C and 1600°C) for one hour, with different percentages of tricalcium phosphate (25 wt%, 50 wt% and 75 wt%). The characterization of the biomaterials was discussed by using differential thermal analysis, dilatometry, X-ray diffraction, ^{31}P magic angle scanning nuclear magnetic resonance, scanning electron microscope and by using the mechanical properties such as rupture strength of different tricalcium phosphate – zirconia composites.

2. Methods and Materials

Synthesized tricalcium phosphate (β-TCP) and commercial zirconia (m-ZrO_2, Fluka, purity 98.5%) powders were mixed with absolute ethanol in an agate mortar. After milling these powders, the mixture (β-TCP and m-ZrO_2) was dried at 80°C for 24 hours. The β-TCP powder was synthesized by solid-state reaction using a mixture of calcium carbonate ($CaCO_3$, Fluka, purity ≥ 99%) and dicalcium phosphate dihydrate ($CaHPO_4.2H_2O$, Fluka, purity ≥ 98%) as the starting materials (I. Sellami *et al*, 2012). Stoechiometric amounts of high purity powders were sintered at 1000°C for three hours, according the following reaction:

$$2\ CaHPO_4.2H_2O_{(s)} + CaCO_{3(s)} \longrightarrow \beta\ Ca_3(PO_4)_{2(s)} + 5\ H_2O_{(g)} + CO_{2\,(g)} \quad (1)$$

The samples were molded in a cylinder having a diameter of 20 mm and a thickness of 6 mm; they were then pressed under 150 MPa. To ensure their reliability, all tests were performed six times under the same conditions.

The heat treatment of the green bodies was carried out in a vertical resistance furnace (Pyrox 2408) at various temperatures between 1100°C and 1600°C for different sintering times (15 min, 30 min, 60 min, 90 min, and 180 min). The heating and cooling rates of the temperature were 10°C/min and 20°C/min, respectively.

The X-ray diffraction (XRD) patterns of the samples were recorded by a Seifert XRD 3000 TT diffractometer, using monochromated CuK_α radiation (λ = 1.54056 Å). To determine the phases present in the samples, XRD peak positions were compared with the International Center for Diffraction Data (ICDD) files.

The magic angle spinning nuclear magnetic resonance (MAS-NMR) spectra were registered by high resolution solid state MAS-NMR (BRUKER 300WB) with a ^{31}P frequency of 121.5 MHz, 5 µs pulse duration, spinning speed of 8000 Hz and a delay of 5s. The ^{31}P shift was given in parts per million (ppm), referenced to 85 wt% H_3PO_4.

Differential thermal analysis (DTA) was carried out using about 30 mg of powder in helium (Setaram SETSYS Evolution 1750). The heating rate was 10°C min^{-1} in an interval of temperature between the ambient temperature and 1500°C. Linear shrinkage was determined by dilatometry (Setaram TMA 92 dilatometer) using the same thermal cycle as the one used for DTA analysis.

The Brunauer-Emmett-Teller (BET) gas adsorption measurement technique was used to measure the specific surface areas (SSA) of the powders, using N_2 as an adsorption gas (ASAP 2020) (S. Brunauer *et al*, 1938). This characterization was carried out after the vacuum degassing at 100°C during three hours. By assuming the primary particles to be spherical, the particle diameter (D_{BET}) was derived from this formula (D. Bernache-Assollant, 1993):

$$D_{BET} = \frac{6}{S\rho} \quad (2)$$

where ρ is the theoretical density of each compound and S is the SSA.

The microstructure of the sintered compacts was investigated on samples of the fractured surfaces with a scanning electron microscope (SEM) (Philips XL 30). These samples were coated with a gold layer for more electronic conductivity.

The mechanical properties of the sintered samples were evaluated using a compressive test. The Brazilian test was used to measure the rupture strength (or mechanical strength) of the sintered compacts (ISRM, 1987; ASTM C496, 1984). Brazilian tests or splitting tests consist of crushing a bedded cylindrical specimen between two crushing plates (ISRM, 1978; ASTM C496, 1984). The usual way of evaluating the tensile strength obtained from the diametrical compression test is by using equation (3).

$$\sigma_r = \frac{2 \times P}{\Pi \times D \times t} \quad (3)$$

Where P is the maximum applied load, *D* is the diameter and t is the thickness of the sample.

The experiments were realized by using a LLOYD EZ50 device on cylindrical samples of approximately 6 mm in thickness and 20 mm in diameter.

3. Results and discussion

3. 1. Characterization of the different powders

Table 1 summarizes the SSA; the average grain size (D_{BET}) determined by equation (2) and the average grain size obtained by granulometric repartition (D_{50}) for the powders used in this work (TCP and ZrO_2). These D_{BET} values obtained by SSA do not correspond to those obtained from granulometric repartition (Table 1). The discrepancy between those values may be due to the presence of agglomerates which are formed during the preparation of the TCP powder at 1000°C.

Table 1 Characteristics of powders used in this study.

Compounds	SSA (m^2/g) (± 1.0)	D_{BET} (µm) (± 0.2)	D_{50} (µm)[a] (± 0.2)
TCP	2.25	0,86	6
m-ZrO_2	2.60	0,40	5

[a] Mean diameter.

The XRD pattern obtained from the initial β-TCP powder, which is obtained from the solid state reaction process, is reported in Figure 1a. The X-ray diffraction phase analysis reveals only the β-tricalcium phosphate (ICDD data file no. 09-0169) without any other structure. All the diffraction peaks, illustrated in Figure 1b, correspond to the monoclinic zirconia: m-ZrO_2 (ICDD data file no. 37-1484).

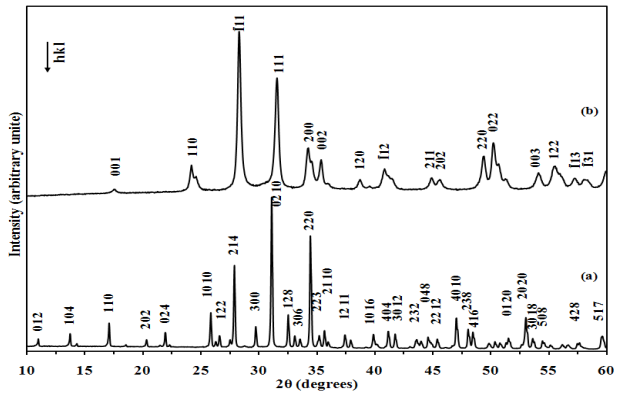

Figure 1 XRD patterns of (a) β-TCP powder, and (b) m-ZrO_2 powder

The ^{31}P MAS-NMR solid analysis of the TCP and the different TCP-ZrO_2 composites are shown in Figure 2. These spectra reveal the presence of the tetrahedral environments of phosphorus ^{31}P. This result is similar to those previously proved by Destainville *et al*. and Bouslama *et al*. (A. Destainville *et al*, 2003; N. Bouslama *et al*, 2010). Indeed, they confirm that the phosphorus atoms of tricalcium phosphate are located in three crystallographic sites: $P(1)O_4$, $P(2)O_4$ and $P(3)O_4$ (A. Destainville *et al*, 2003).

Figure 3 illustrates the differential thermal analysis curves of the tricalcium phosphate, zirconia and the different TCP-ZrO_2 composites. The DTA curve of the zirconia powder is presented in Figure 3a. An endothermic peak, observed at 1170°C, is linked to the allotropic transformation of zirconia from the monoclinic phase (m) to the tetragonal phase (t) (Figure 3a). The DTA curve of the tricalcium phosphate identified three endothermic peaks (Figure 3e). The first peak, at 190°C, is linked to dehydration. A second peak, around 1290°C, characterizes the first allotropic transformation of tricalcium phosphate: β to α. The last peak towards 1460°C corresponds to the second allotropic transformation of TCP (α to α'). The DTA curves of the different TCP-ZrO_2 composites showed only an endothermic peak at 1460°C which is related to the allotropic transformation of TCP (α to α') (Figures 3b-3d). In these curves, the endothermic peak relative to the first allotropic transformation of TCP has practically disappeared (Figures 3b-3d). This result can probably be explained by the presence of zirconia in the TCP compound.

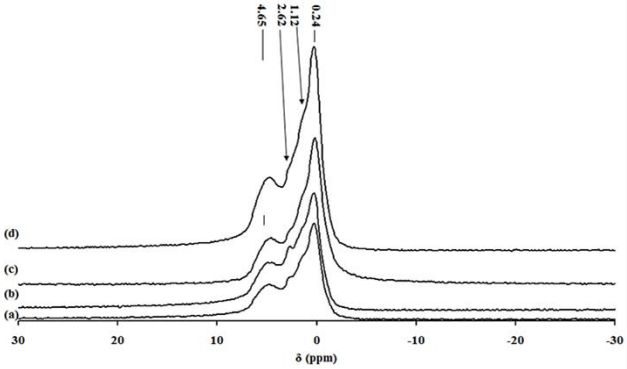

Figure 2 ^{31}P MAS-NMR spectra of powder (a) TCP-25 wt% ZrO2 composites, (b) TCP-50 wt% ZrO2 composites, (c) TCP-75 wt% ZrO2 composites and (d) β-TCP

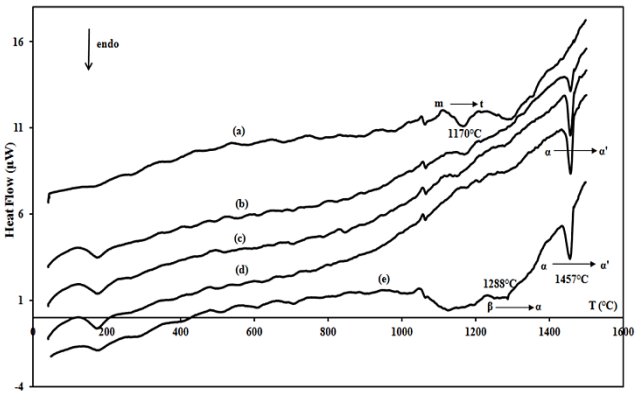

Figure 3 DTA curves of (a) ZrO_2, (b) TCP-75 wt% ZrO_2 composites, (c) TCP-50 wt% ZrO_2 composites, (d) TCP-25 wt% ZrO_2 composites and (e) TCP

Dilatometry analysis was carried out on the different powders used in this study to evaluate their extent of shrinkage in the temperature range from ambient temperature to 1400°C (Figure 4). The sintering process began at about 1106°C, 1120°C, 1110°C, 1125°C and 1120°C for the β-TCP, ZrO_2, TCP-25 wt% ZrO_2 composites, the TCP-50 wt% ZrO_2 composites and the

TCP-75 wt% ZrO_2 composites, respectively. Table 2 summarizes the range of the sintering temperatures of the different powders. The addition of TCP in the ZrO_2 matrix decreases the sintering temperature of the different TCP-ZrO_2 composites (Table 2). We can then say that the addition of TCP decreases the sintering temperature of the pure ZrO_2. During the cooling step from 910°C to 830°C, the DTA curves of zirconia and the different TCP-ZrO_2 composites show the expansion in volume which is relative to the inverse allotropic transformation from the tetragonal phase to the monoclinic phase of zirconia (Figures 4a-4c). In fact, the tetragonal phase has a higher density (6.10 g/cm^3) than the monoclinic phase (5.83 g/cm^3). It can be noticed that the expansion in volume of the samples decreases when the percentage of TCP increases in the TCP-ZrO_2 composites (Figures 4b-4d). The curve of the TCP-25 wt% ZrO_2 composites shows no expansion in volume (Figure 4d). Thus, the addition of the 75 wt% TCP in the ZrO_2 reduces this expansion completely (Figure 4d). So, the addition of TCP may stabilize the zirconia structure and prevent this expansion in volume which is responsible for the fragility of the zirconia compounds (Figures 4a-4d). In fact, it is possible to stabilize the zirconia structure by adding TCP. Thus, the addition of TCP in the zirconia matrix prevents the inverse allotropic transformation of zirconia and enhances the contraction of the zirconia samples. At 1290°C, the speed behavior in the TCP curve changes because of to the β - α transformation of tricalcium phosphate (Figure 4e).

Table 2 Range of the sintering temperature and the theoretical density of various compounds.

Compounds	$d_{théo}$ [a]	Range of sintering (°C)	shrinkage (%)
m-ZrO_2	5.83	[1000-1388]	3
TCP-75 wt% ZrO_2 composites	5.14	[975-1388]	5.34
TCP-50 wt% ZrO_2 composites	4.45	[980-1384]	6.6
TCP-25 wt% ZrO_2 composites	3.76	[976-1384]	8.45
TCP	3.07 (β) 2.86 (α)	[950-1384]	11.7

[a] Theoretical density

3. 2. The mechanical properties of the tricalcium phosphate

Figure 5 illustrates the evolution of the mechanical strength of β-TCP sintered for one hour at various temperatures (between 1100°C and 1500°C). The mechanical strength of the tricalcium phosphate increased with the sintering temperature (Figure 5). Between 1100°C and 1300°C, the mechanical properties were practically constant, between 0.4 MPa and 0.5 MPa. At 1350°C, the mechanical properties of TCP reached maximum value around 8 MPa. Above 1350°C, the mechanical properties of TCP decreased abruptly (Figure 5).

Figure 6 shows the mechanical strength of tricalcium phosphate sintered at 1350°C with different sintering periods. The mechanical strength of TCP increased with the sintering period until an optimum of nearly 8 MPa was obtained for the samples sintered at 1350°C for 60 minutes (Figure 6).

The results obtained show that the tricalcium phosphate presents a good rate of mechanical strength after the sintering process at 1350°C. In fact we can notice that the rupture strength of about 8 MPa could be reached at 1350°C. This result was previously confirmed by Bouslama *et al*. showing that the mechanical strength of tricalcium phosphate increases with the temperature until it achieves 5 MPa at 1320°C (N. Bouslama *et al*, 2009). In addition, Sakka *et al*. found that the mechanical strength of TCP reached its optimum value (4 MPa) at 1350°C (S. Sakka *et al*, 2012). Thus, the result we found with the Brazilian test was in concordance with the earlier results proved by the literatures (N. Bouslama *et al*, 2009; S. Sakka *et al*, 2012).

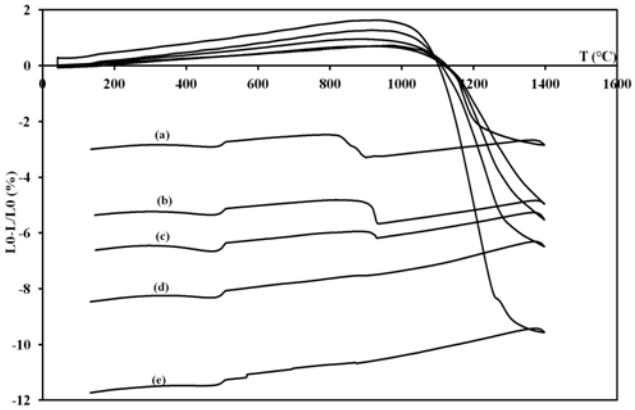

Figure 4 Linear shrinkage relative to the temperature of (a) ZrO_2, (b) TCP-75 wt% ZrO_2 composites, (c) TCP-50 wt% ZrO_2 composites, (d) TCP-25 wt% ZrO_2 composites and (e) TCP

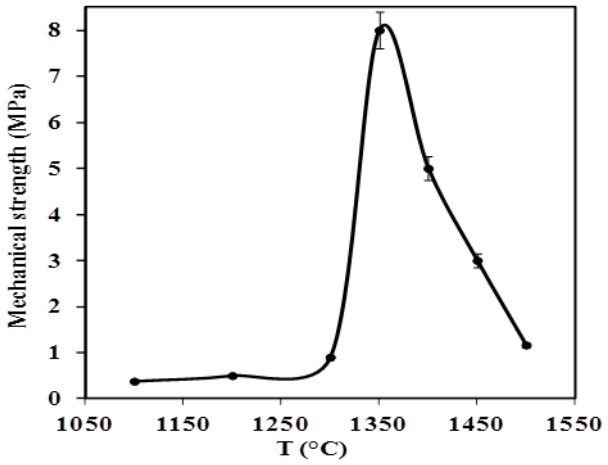

Figure 5 Mechanical strength of the TCP sintered for one hour versus the sintering temperature

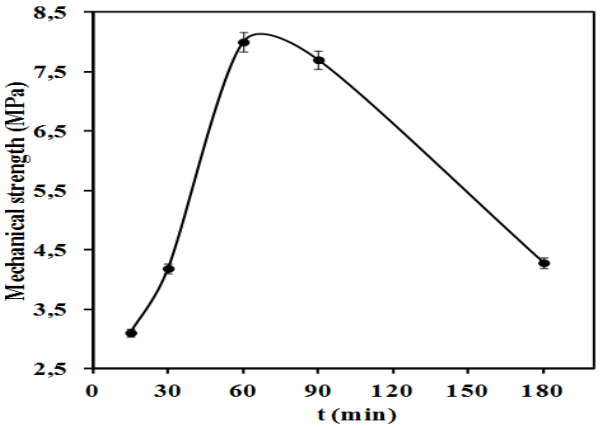

Figure 6 Mechanical strength of the TCP sintered at 1350°C for different sintering times

3. 3. The mechanical properties of the TCP-ZrO_2 composites

Figure 7 reports the evolution of the mechanical strength of the TCP-ZrO_2 composites, sintered between 1300°C and 1600°C with different percentages of TCP (25 wt%, 50 wt% and 75 wt%). Pure zirconia has a low mechanical strength (Figure 7a). Indeed, the ultimate mechanical strength of pure zirconia reached 2.8 MPa at 1400°C (Figure 7a). This low mechanical strength of pure zirconia is due to the inverse allotropic transformation from the tetragonal phase to the monoclinic phase of zirconia. This transformation is responsible for the fragility of the zirconia samples. The mechanical strength of the TCP-ZrO_2 composites increases with the percentages of TCP. The optimum value of the mechanical properties of the TCP-ZrO_2 composites (6 MPa) was obtained at 1600°C with 25 wt% TCP (Figure 7b). The evolution of the mechanical properties of the TCP-25 wt% ZrO_2 composites was practically similar to that of the TCP-50 wt% ZrO_2 composites (Figures 7b and 7c). Table 3 summarizes the optimum values of the mechanical strength of the different TCP-ZrO_2 composites sintered for one hour at various temperatures. This study reveals that the addition of TCP enhances the mechanical strength of zirconia.

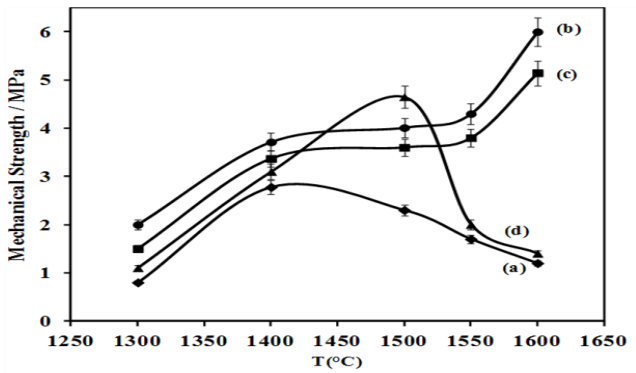

Figure 7 Mechanical strength of the TCP-ZrO_2 composites sintered for one hour versus the sintering temperature with different amounts of TCP: (a) 0 wt%, (b) 25 wt%, (c) 50 wt% and (d) 75 wt%

The influence of the sintering temperature on the mechanical properties of TCP-ZrO_2 composites was investigated. The experimental results indicate the appearance of low mechanical properties of pure zirconia. The mechanical strength is ameliorated after the sintering process of zirconia at 1600°C with 25 wt% TCP. Table 4 displays several examples of the mechanical strength of TCP, ZrO_2 and the bone tissues (P. Ducheyne *et al*, 1981); (C. Lavernia *et al*, 1991); (L.L. Hench, 1991); (L.L. Hench, 1993); (J. Li *et al*, 1993); (Y.J. Horng *et al*, 1994); (JC. Elliott, 1994); (L.L. Hench, 1998); (N. Bouslama *et al*, 2010); (F. Ben Ayed, 2011); (S. Sakka *et al*, 2012) and (I. Sellami *et al*, 2012). The obtained rupture strength of the TCP-75 wt% ZrO_2 composites (6 MPa) is within the values reported in the literature (2 – 12 MPa) (Table 4). Moreover, the wide variation in the mechanical properties of the samples reported in the literature is due to the synthesis methods of the β-TCP powder, the size of the particles and the application of different processing parameters. Generally, the values found for the mechanical properties of our TCP-ZrO_2 composites are not identical to those in Table 4, because the authors have used different mechanical modes other than the Brazilian test.

Table 3 Evolution of the mechanical properties of different TCP-ZrO_2 composites.

Compounds	σ_r[a] (MPa)	T[b] (°C)
m-ZrO_2	3.8	1450
TCP-75 wt% ZrO_2 composites	6	1600
TCP-50 wt% ZrO_2 composites	5.14	1600
TCP-25 wt% ZrO_2 composites	4.6	1500

[a] Mechanical resistance
[b] Sintering temperature

Table 4 Examples from the literature of the mechanical properties of the TCP, the ZrO_2 and the bone tissues.

	σ_r[a] (MPa)	References
β-TCP	4 − 8	(S. Sakka et al, 2012) (I. Sallemi et al, 2012)
ZrO_2	2 − 4	(C. Yamagata *et al*, 2011) (S. Arnaud et al, 2011)
Cortical bone	130 − 180	(L.L. Hench, 1993) (JC. Elliott, 1994)
Cancellous bone	2 − 12	(L.L. Hench, 1993) (JC. Elliott, 1994)
Enamel	8 − 12	(C. Lavernia et al, 1991) (L.L. Hench, 1998)
Dentin	45 − 55	(C. Lavernia et al, 1991) (L.L. Hench, 1998)

[a] mechanical strength

3. 4. Characterization of the samples after the sintering process

After the sintering process, the samples have been characterized through different techniques such as X-ray diffraction (XRD), ^{31}P nuclear magnetic resonance (MAS-NMR) and scanning electron microscope (SEM).

The X-ray diffraction analyses of the TCP-ZrO_2 composites heated at various temperatures (1300°C, 1400°C and 1500°C) for one hour are presented in Figure 8. The XRD patterns of the samples sintered at 1300°C show the presence of α-TCP phase (ICDD data files no. 09-348) besides the initial phase (Figure 8). In addition to the phases mentioned earlier, the XRD patterns of the samples sintered above 1400°C reveal the presence of traces of tetracalcium phosphate ($Ca_4(PO_4)_2O$, TTCP) (ICDD data files no. 70-1379) (Figure 8). We conclude that the X-ray diffraction analysis reveals the formation of a new phase of the tetracalcium phosphate for temperatures higher than or equal to 1400°C. The same result was found previously by Ben Ayed *et al*. (F. Ben Ayed *et al*, 2008). The latter show that during the study of the sintering of the tricalcium phosphate – fluorapatite - zirconia composites, the percentage of tetracalcium phosphate increased above 1300°C for high mass percentages of zirconia (superior or equal to 20%) (F. Ben Ayed *et al*, 2008). Similarly, the presence of TTCP is observed by Khor *et al*. during the study of the effects of ZrO_2 on the phase compositions plasma sprayed Hap-YSZ composites coatings (K.A. Khor *et al*, 2003).

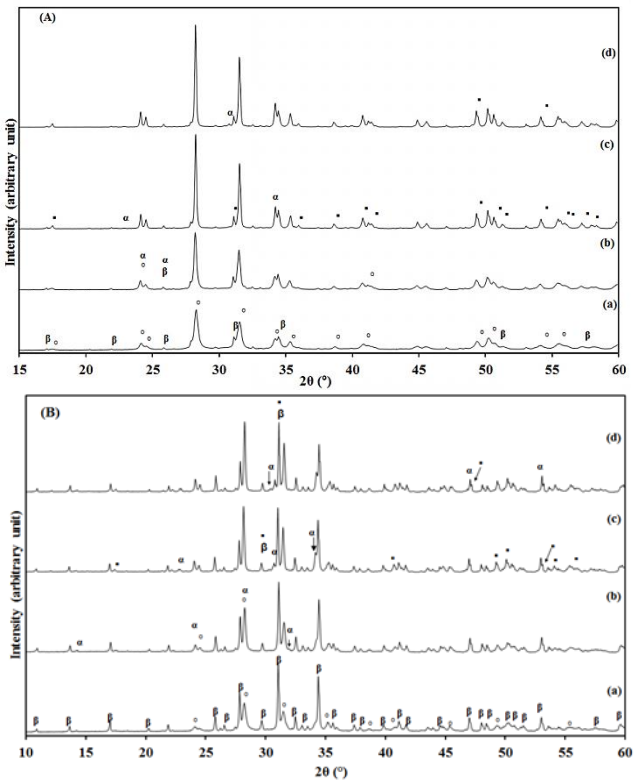

Figure 8 XRD patterns of the TCP-ZrO_2 composites sintered at various temperatures for one hour with different amounts of TCP : (A) 25 wt%, (B) 75 wt%; (a) raw, (b) 1300°C, (c) 1400°C and (d) 1500°C (β : β-$Ca_3(PO_4)_2$; ° : m-ZrO_2 ; α : α-$Ca_3(PO_4)_2$; ▪ : $Ca_4(PO_4)_2O$).

Figure 9 shows the ^{31}P MAS-NMR spectra of the TCP-ZrO_2 composites sintered for one hour at various temperatures (1300°C, 1400°C, 1500°C and 1600°C) (Figures 9A–9C). All curves indicate the presence of tetrahedral environments. These environments are assigned to phosphorus (Q^1 type).

The typical microstructures of the TCP-ZrO_2 composites were observed by SEM analysis after the sintering process at various temperatures (1500°C and 1600°C) (Figure 10). These microstructures corroborate the evolution of the mechanical properties of the TCP-ZrO_2 composites with the sintering temperatures and with different percentages of TCP (25 wt%, 50 wt% and 75 wt%). The microstructural investigations of the TCP-ZrO_2 composites sintered at various temperatures (1500°C and 1600°C) with 25 wt% TCP shown in Figures 10a and 10b. At 1500°C, the grains of zirconia are well clustered in the grain boundaries of TCP (Figure 11a). At 1600°C, an exaggerated enlargement of the grains was observed with an intragranular porosity of about 6 µm (Figure 11b). An increase of the percentage of TCP from 25 wt% to 50 wt% in the TCP-ZrO_2 composites results in a significant change of the microstructure. Indeed, we notice a continuous matrix and closed macro porosity in the order of 12 µm at 1600°C (Figures 10c, 10d). In the presence of 75 wt% TCP, the TCP-ZrO_2 composites sintered at 1500°C contain an important intragranular porosity (Figure 10e). At 1600°C, the microstructure of TCP-25 wt% ZrO_2 composites reveals the formation of a liquid phase that can take place with the increase of the sintering temperature and the increase of the amount of TCP (Figure 10f). In fact, it is evident that an increase in mechanical properties is achieved by increasing the sintering temperature because the presence of the liquid phase helps to fill the pores and enhances the mechanical properties. This result was previously proven by the literatures (F.H. Perera *et al*, 2010; S. Sakka *et al*, 2012). Additionally, at 1600°C, the mechanical properties of the TCP-25 wt% ZrO_2 composites were hindered by the existence of large pores of about 7 µm and by the formation of some micro-cracks (Figure 10f). The occurrence of the micro-cracks may be attributed to the allotropic transformation of TCP. This is due to the expansion-contraction cycle generated by the differences in density between β-TCP (3.07 g/cm^3) and α-TCP (2.86 g/cm^3). This phenomenon was previously detected by the literatures (K. Lin *et al*, 2007); (F. Ben Ayed *et al*, 2007); (F. Ben Ayed *et al*, 2008); (P. Miranda *et al*, 2008); (N. Bouslama *et al*, 2009); and (F.H. Perera *et al*, 2010). In fact, Bouslama *et al*. and Perera *et al*. also observed this result in their studies (N. Bouslama *et al*, 2009; F.H. Perera *et al*, 2010). Furthermore, at 1600°C, the micrograph of the TCP-25 wt% ZrO_2 composites indicates a better coalescence of grains of zirconia (Figure 10f). This result was generally due to the stabilization of the zirconia phase by the addition of TCP.

In this study, the rupture strength of the TCP-ZrO_2 composites attained its ultimate value after the sintering

process at 1600°C for one hour with 25 wt% TCP. This result is obtained by the stabilization of the zirconia phase with the addition of TCP. Moreover, at a high temperature, the presence of the liquid phase of the TCP phase helps to fill the pores and enhances the mechanical performance of the zirconia samples. SEM analyses of the TCP-ZrO_2 composites show that a differential increase in the grain size takes place with the increase of the amounts of TCP (Figure 10f). According to the literature, the inclusion of zirconia at the level of the grain boundaries reduced the exaggerated enlargement of the grains of TCP, as it was mentioned earlier by Horng *et al*. in their study concerning the elaboration and the mechanical properties of the hydroxyapatite – bioinert oxides composites (Y.J. Horng, 1994).

The partially reaction of TCP with ZrO_2 can be explained as resulting from removal of calcium from the TCP and its dissolution into the zirconia. This result was previously confirmed by Zafer during of the study of the sintering of the TCP-ZrO_2 composites (E. Zafer, 2007). In fact, he shows that, the exchange of Ca^{2+} and ZrO^{2+} ions can occur where the surfaces of ZrO_2 and Hap are in contact, with minimum rearrangement of their structures.

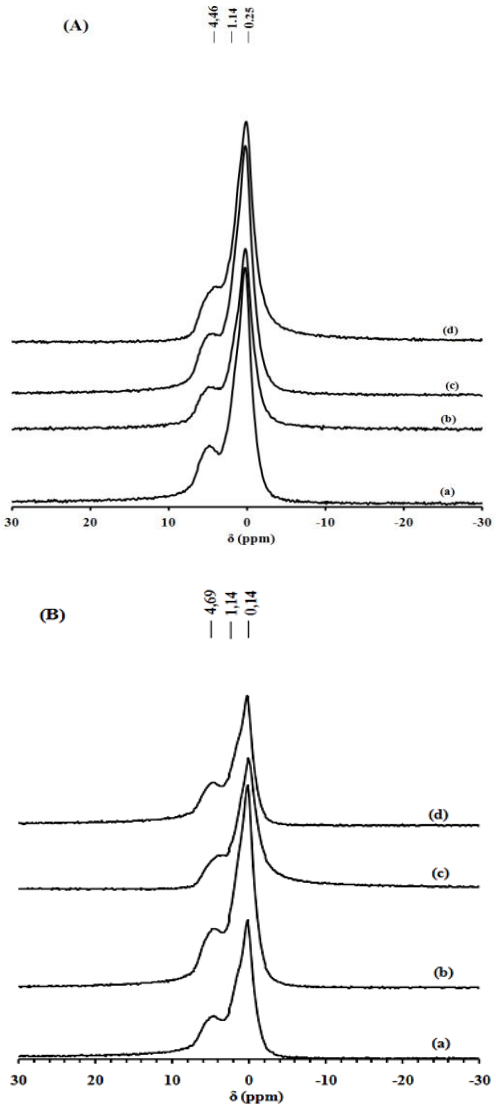

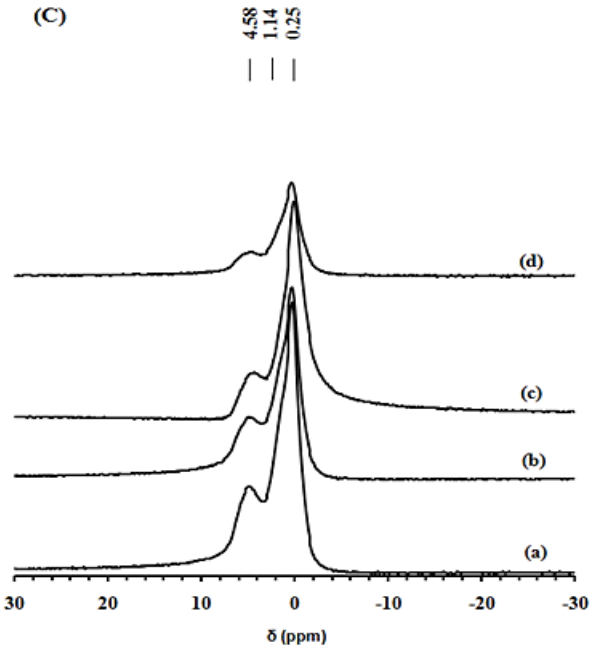

Figure 9 ^{31}P MAS-NMR spectra of the TCP-ZrO_2 composites sintered at various temperatures for one hour with different amounts of TCP: (A) 25 wt%, (B) 50 wt% and (C) 75 wt%; (a) 1300°C, (b) 1400°C, (c) 1500°C and (d) 1600°C.

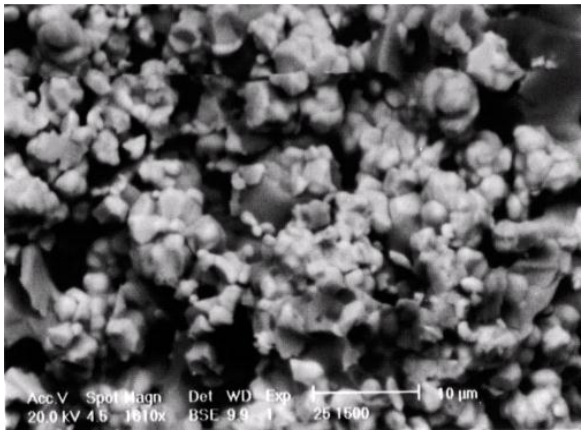

(a)

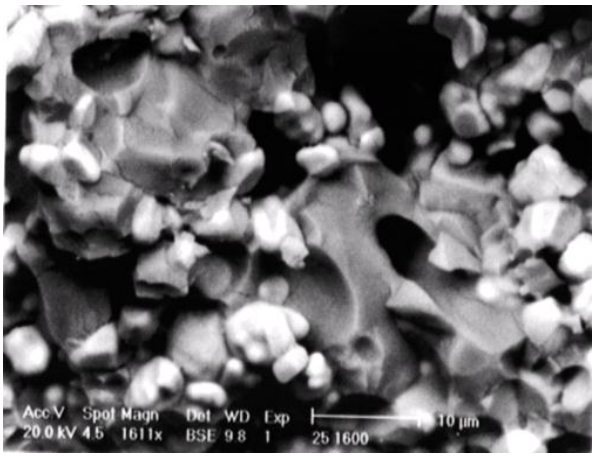

(b)

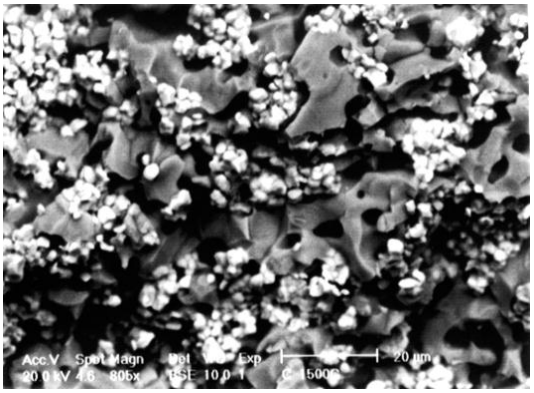

(c)

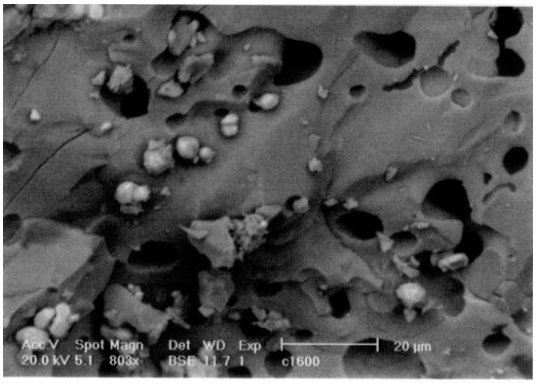

(d)

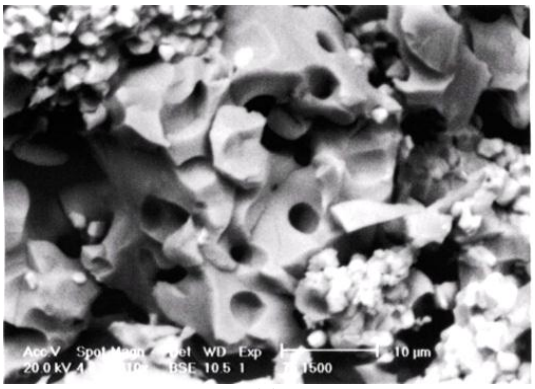

(e)

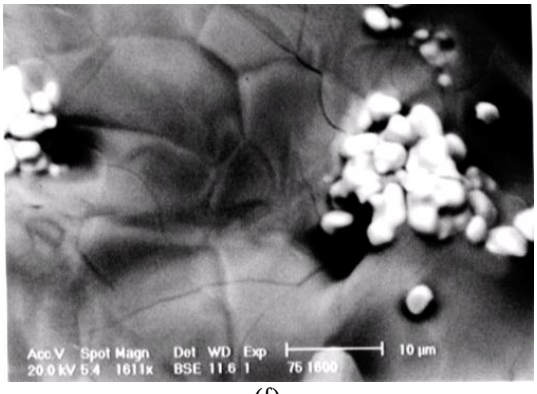

(f)

Figure 10 SEM micrographs of the TCP-ZrO_2 composites sintered for one hour at various temperatures with different percentages of TCP : (a) 25 wt%, 1500 °C; (b) 25 wt%, 1600 °C; (c) 50 wt%, 1500 °C; (d) 50 wt%, 1600 °C; (e) 75 wt%, 1500 °C and (f) 75 wt%, 1600 °C

Three series of powders of tricalcium phosphate-zirconia composites with different TCP contents (25 wt%, 50 wt% and 75 wt%) were sintered between 1300 and 1600°C for one hour. Based on the results we discussed earlier, it emerges that the inverse allotropic transformation of zirconia is sufficient to cause the degradation of its mechanical properties. This phenomenon was also studies by Subbarao *et al*. and Arnaud *et al*. (E.C. Subbarao *et al*, 1981; S. Arnaud *et al*, 2011). The partially stabilized zirconia has been widely studied due to its high strength and fracture toughness (E.C. Subbarao *et al*, 1981); (P. Christel *et al*, 1989); (S. Arnaud *et al*, 2011); (C. Yamagata *et al*, 2011) and (O. Vasykir *et al*, 2003). Several stabilizing oxides, such as yttria (Y_2O_3) among others, were added in order to prevent the inverse allotropic transformation of zirconia (C. Yamagata *et al*, 2011 ; O. Vasykir *et al*, 2003). Yamagata *et al*. show that yttria degrades the tetragonal zirconia at low temperatures, especially when exposed to humid environments (C. Yamagata *et al*, 2011). Thus, the transformation of the tetragonal phase to the monoclinic phase occurs because of the reaction of water with the tetragonal grains of zirconia (C. Yamagata *et al*, 2011). Vasykir *et al*. show that the 3-mol%-yttria stabilizes tetragonal zirconia at low sintering temperature also (O. Vasykir *et al*, 2003). But the yttria compound is not a biomaterial and is not biocompatible with the bone tissues (O. Vasykir *et al*, 2003). In the light of this consideration, we have chosen β-TCP as the agent of stabilization to be added to zirconia. An extensive study of the effect of the addition of TCP on the phase transformation, the stability, the rupture strength and the microstructures of zirconia was discussed. In fact, β-TCP has an excellent biocompatibility in the human body and a better resorbability in vivo with new bone growth (F. Ben Ayed *et al*, 2001; H. K. Varma *et al*, 2001 ; R. Rao. Ramachandra *et al*, 2002 ; H.S. Ryu *et al*, 2002; Yashima *et al*, 2003; A. Destainville *et al*, 2003 ; C.X. Wang *et al*, 2004; S. Hoell *et al*, 2005; R.D. Gaasbeek *et al*, 2005; S.S. Jensen *et al*, 2006; J. Chevalier, 2006; F. Ben Ayed *et al*, 2006; A.K. Guha *et al*, 2009; F.H. Perera *et al*, 2010; N. Bouslama *et al*, 2010; F. Ben Ayed, 2011; A. Guidera *et al*, 2011; S. Sakka *et al*, 2012; I. Sellami *et al*, 2012; I. Levin *et al*, 1998). The resorbability property imparts significant advantages to TCP compared to other materials, such as yttria, which are not resorbable and cannot be replaced by natural bone (L.L. Hench, 1993; J. Li *et al*, 1993; Y.J. Horng *et al*, 1994; JC. Elliott, 1994; L.L. Hench, 1998; I. Levin *et al*, 1998; E. Landi *et al*, 2000; F. Ben Ayed *et al*, 2000; F. Ben Ayed *et al*, 2001; H. K. Varma *et al*, 2001 ; R. Rao. Ramachandra *et al*, 2002 ; H.S. Ryu *et al*, 2002; Yashima *et al*, 2003; A. Destainville *et al*, 2003 ; C.X. Wang *et al*, 2004; S. Hoell *et al*, 2005; R.D. Gaasbeek *et al*, 2005; S.S. Jensen *et al*, 2006; J. Chevalier, 2006; F. Ben Ayed *et al*, 2006; M. Gutierres *et al*, 2007; G.L. DeSilva *et al*, 2007; K. Lin *et al*, 2007; F. Ben Ayed *et al*, 2007; F. Ben Ayed *et al*, 2008; P. Miranda *et al*, 2008; N. Bouslama *et al*, 2009; J. Chevalier *et al*, 2009 ; K. Chaari *et al*, 2009; A.K. Guha *et al*, 2009; F.H. Perera *et al*, 2010; N. Bouslama *et al*, 2010; F. Ben Ayed, 2011; A. Guidera *et al*, 2011; S.

Sakka *et al*, 2012; I. Sellami *et al*, 2012; E.C. Subbarao *et al*, 1981; P. Christel *et al*, 1989; D.S. Metsger *et al*, 1999; K. Prabakaran *et al*, 2005; E. Zafer, 2007; S. Arnaud *et al*, 2011). As expected, the introduction of TCP in zirconia leads to an increase in the mechanical strength of composite materials.

In our study, the mechanical properties of zirconia increased with the addition of 25 wt% TCP. The presence of the TCP in the zirconia matrix not only enhanced the sintering process but also controlled and partially prevented the inverse allotropic transformation of zirconia. This inverse transformation of the tetragonal phase to the monoclinic phase is responsible for the low values of the rupture strength of the pure zirconia samples. As a result, significant enhancements in the mechanical strength of ZrO_2 were achieved when a 25 wt% amount of TCP was added.

4. Conclusion

Tricalcium phosphate and zirconia powders were mixed in order to elaborate bioceramics composites for biomedical applications. The addition of TCP in the ZrO_2 matrix has drawn much attention due to its biocompatibility coupled with the tendency to enhance the mechanical properties of ZrO_2. The maximum of mechanical strength of the tricalcium phosphate - 75wt% zirconia composites was obtained at 1600°C. These results prove the stabilization of the structure of zirconia with the addition of the tricalcium phosphate. Thus, the addition of the TCP in the zirconia matrix partially prevents the inverse allotropic transformation of zirconia and enhances the contraction of the zirconia. This result was explained by the exchange of Ca^{2+} and ZrO^{2+} between the TCP and ZrO_2. High mass percentages of TCP (near 75 wt %) are not the best conditions for the mechanical properties of the TCP - zirconia composites. This is probably due to the new compound formation (TTCP).

References

A. Destainville, E. Champion, and D. Bernache – Assolant, (2003), Characterization and thermal behavior of apatitic tricalcium phosphate, *Mater Chem Phys.*, Vol. 80, p. 269.

A. Guidera, K. Chaari, and J. Bouaziz, (2011), Elaboration and Characterization of Alumina-Fluorapatite Composites, *J Biomat Nano.*, Vol. 2, pp.103-113.

A.K. Guha, S. Singh, R. Kumarresan, S. Nayar, and A. Sinha, (2009), *Coll. Surf. B: Biointerface*, Vol. 73, pp.146–151.

ASTM C496, (1984), Standard test method for splitting tensile strength of cylindrical concrete specimens , *Annual Book of ASTM Standards*, Vol. 42, p.336.

C. Lavernia, and J.M. Schoenung, (1991), Calcium phosphate ceramics as bone substitutes, *Am Ceram Soc Bull.*, Vol. 70, pp. 95-100.

C.X. Wang, X. Zhou, and M. Wang, (2004), Influence of sintering temperatures on hardness and Young's modulus of tricalcium phosphate bioceramic by nanoindentation technique, *Mat Charac*., Vol. 52, p.301.

C. Yamagata, and P. J. Octavio Armani, (2011), Influence of Y2O3 Addition on the Microstructure and Mechanical Properties of Mg-PSZ Ceramics, *J Mat Sci Eng A*, Vol. 1, pp.556–561.

D. Bernache-Assollant, (1993), Chimie-physique du frittage, Editions Hermès.

D.S. Metsger, M.R. Rieger, and D.W. Foreman, (1999), Mechanical properties of sintered hydroxapatite and tricalcium phosphate ceramic, *J Mater Sci Mater Med*.,Vol. 10, pp.9–17.

E.C. Subbarao, (1981), Science and technology of zirconia , in advances in ceramics, *Amer Ceram Soc.*, Vol. 3 Ed.A.H. Heuer and L.W. Hobbs, pp. 1–24.

E. Landi, A. Tampieri, G. Celotti, and S. Sprio, (2000), Densification Behavior and Mechanisms of Synthetic Hydroxyapatites, *J Eur Ceram Soc*., Vol. 20, pp. 2377-2387.

E. Zafer, (2007), Reactions in Hydroxylapatite-Zirconia Composites, *Ceram Inter.*, Vol. 33, pp. 987–991.

F. Ben Ayed, Biomaterials - Physics and Chemistry, In: Rosario Pignatello, Editor.ISBN 978-953-307-418-4, Chapter 18: Elaboration and characterisation of calcium phosphate biomaterial for biomedical application, Publishing In Tech, Croatia (2011) 357–374.

F. Ben Ayed, and J. Bouaziz, (2007), Elaboration and characterisation of calcium phosphate biomaterial, *C R Phy*., Vol. 8, pp. 101−108.

F. Ben Ayed, J. Bouaziz, (2008), Sintering of tricalcium phosphate–fluorapatite composites by addition of alumina, *Ceram Int.*, Vol. 34, pp. 1885−1892.

F. Ben Ayed, J. Bouaziz, (2008), Sintering of tricalcium phosphate–fluorapatite composites with zirconia, *J Eur Ceram Soc.*, Vol. 28, pp. 1995−2002.

F. Ben Ayed, J. Bouaziz, K. Bouzouita, (2000), Pressureless sintering of fluorapatite under oxygen atmosphere, *J Eur Ceram Soc*, Vol. 20, p. 1069.

F. Ben Ayed, J. Bouaziz, I. Khattech, K. Bouzouita, (2001), Produit de solubilité apparent de la fluorapatite frittée, *Ann Chim Sci Mater*., Vol. 26, p. 75.

F. Ben Ayed, J. Bouaziz, K. Bouzouita, (2001), Calcination and sintering of fluorapatite under argon atmosphere, *J Alloys Compd*., Vol. 322, p. 238.

F. Ben Ayed, J. Bouaziz, K. Bouzouita, (2006), Résistance mécanique de la fluorapatite, *Ann Chim Sci Mater.*, Vol. 31, p. 393.

F. Ben Ayed, K. Chaari, J. Bouaziz, K. Bouzouita, (2006), Frittage du phosphate tricalcique, *C R Phy*., Vol. 7, pp. 825-835.

F.H. Perera, F.J. Martinez-Vazquez, P. Miranda, A.L. Ortiz, A. Pajares, (2010), Clarifying the effect of sintering conditions of the microstructure and mechanical properties of beta-tricalcium phosphate, *Ceram Inter.*, Vol. 36, pp.1929–1935.

G.L. DeSilva, A. Fritzler, S.P. DeSilva, (2007), Antibiotic-impregnated cement spacer for bone defects of the forearm and hand, *Tech Hand UpExtrem Surg.*, Vol. 11, pp. 163–167.

H. K. Varma, S. Sureshbabu, (2001), Oriented growth of surface grains in sintered beta tricalcium phosphate bioceramics, *Mat let*., Vol. 49, pp.83−85.

H.S. Ryu, H.J. Youn, K.S. Hong, B.S. Chang, C.K. Lee, S.S. Chung, (2002), An improvement in sintering property of beta-tricalcium phosphate by addition of calcium pyrophosphate, *Biomaterials*, Vol. 23, pp. 909–914.

I. Levin, D. Brandon, (1998), Metastable Alumina Polymorphs: Crystal Structures and Transition, *J Am Ceram Soc.*, Vol. 81, pp. 1995–2012.

I. Sellami, F. Ben Ayed, J. Bouaziz, (2012), Effect of fluorapatite additive on the mechanical properties of tricalcium phosphate-zirconia composites, *IOP Conf Series: Mat Sc Eng*., Vol. 28, p. 012029.

ISRM, (1978), Suggested methods for determining tensile strength of rock materials, *Int J Rock Mech Min Sci Geomech Abstr.*, Vol. 15, pp. 99–103.

JC. Elliott, Structure and Chemistry of the Apatite and Other Calcium Orthophosphates, Elsevier Science B.V., Amsterdam (1994).

J. Li, L. Hermansson, R. Soremark, (1993), High-Strength Biofunctional Zirconia: Mechanical Properties and Static Fatigue

Behaviour of Zirconia-Apatite Composites, *J Mater Sci Mat Med*., Vol. 4, pp. 50–54.

J. Chevalier, (2006), What future for zirconia as a biomaterial, *Biomaterials*, Vol. 27, pp. 535–543.

J. Chevalier, L. Gremillard, (2009), Ceramics for medical applications: a picture for the next 20 years, *J Eur Ceram Soc*., Vol. 29, pp. 1245–1255.

K.A. Khor, H. Li, P. Cheang, (2003), Processing–microstructure–property relations in HVOF sprayed calcium phosphate based bioceramic coatings, *Biomaterials*, Vol. 24, pp. 2233–2243.

K. Chaari, F. Ben Ayed, J. Bouaziz, K. Bouzouita, (2009), Elaboration and Characterization of Fluorapatite Ceramic with Controlled Porosity, *Mat Chem Phy.*, Vol. 113, pp. 219–226.

K. Lin, J. Chang, J. Lu, W. Wu, Y. Zeng, (2007), Properties of beta-Ca3(PO4)2 bioceramics prepared using nano-size powders, *Ceram Inter.*, Vol. 33, pp. 979–985.

K. Prabakaran, S. Kannan, S. Rajeswari, , (2005), Development and characterization of Zirconia and hydroxylapatite composites for orthopedic application, *Trends Biomater Artif Organs*., Vol. 18, pp. 114–116.

L.L. Hench, (1993), An introduction to bioceramics, J. Wilson ed. World Scientific, Singapore.

L.L. Hench, (1991), Bioceramics: From Concept to clinic, *J Am Ceram Soc.*, Vol. 74, pp. 1487−1510.

L.L. Hench, (1998), Bioceramics, *J Amer Ceram Soc*., Vol. 81, pp. 1705−1728.

M. Gutierres, A.G. Dias, M.A. Lopes, N.S. Hussain, A.T. Cabral, L. Almeid, (2007), Openning wedge high tibial osteotomy using 3D biomodelling Bonelike® macroporous structures - case report, *J Mater Sci Mater Med*., Vol. 18, pp. 2377–2382.

N. Bouslama, F. Ben Ayed, J. Bouaziz, (2009), Sintering and mechanical properties of tricalcium phosphate fluorapatite composites, *Ceram Int*., Vol. 35, pp. 1909−1917.

N. Bouslama, F. Ben Ayed, J. Bouaziz, (2010), Effect of fluorapatite additive on densification and mechanical properties of tricalcium phosphate, *J Mech Behav of Biom Mat., Vol.* 3, pp. 2-13.

N. Bouslama, F. Ben Ayed, J. Bouaziz, (2009), Mechanical properties of tricalcium phosphate-fluorapatite alumina composites, *Phy Proce.*, Vol. 2, pp. 1441–1448.

O. Vasykir, Y. Sakka, V.V. Skorohod, (2003), Low temperature processing and mechanical properties of zirconia and zirconia – alumina nanoceramics, *J Am Ceram Soc*., Vol. 86, pp. 299–304.

P. Christel, A. Meunier, M. Heller, J.P. Torre, C.N. Peille, (1989), Mechanical properties and short-term in-vivo evaluation of yttrium-oxide-partially-stabilized zirconia, *J Biomed Mater Res*., Vol. 23, pp. 45–61.

P. Ducheyne, K de Groot, (1981), In vivo surface activity of a hydroxyapatite Alveolar bone substitute, *J Biomed Mater Res*. Vol. 15, pp. 441−445.

P. Miranda, A. Pajares, E. Saiz, A.P. Tomsia, F. Guiberteau, (2008), Mechanical properties of calcium phosphate scaffolds fabricated by robocasting, *J Biomed Mate Res A*, Vol. 85A, pp. 218–227.

R.D. Gaasbeek, H.G. Toonen, R.J. Van Heerwaarden, P. Buma, (2005), Mechanism of bone incorporation of β-TCP bone substitute in open wedge tibial osteotomy in patients, *Biomaterials*, Vol. 26, pp. 6713–6719.

R. Rao. Ramachandra, T.S. Kannan, (2002), Synthesis and sintering of hydroxyapatite – zirconia composites, *Mat Sc Eng C*, Vol. 20, pp. 187–193.

S. Hoell, J. Suttmoeller, V. Stoll, S. Fuchs, G. Gosheger, (2005), The High Tibial Osteotomy, Open Versus Closed Wedge, a Comparison of Methods in 108 Patients, *Arch Trauma Surg*., Vol. 125, pp. 638–643.

S. Arnaud, T. Douillard, C. Cayron, N. Godin, M. R'mili, G. Fantozzi, (2011), Microcracking of high zirconia refractories after t → m phase transition during cooling: An EBSD study, *J Eur Ceram Soc*., Vol. 31, pp. 1525–1531.

S. Brunauer, P.H. Emmet, J. Teller, (1938), Adsorption of Gases in Multimolecular Layers, *J Am Chem Soc*., Vol. 60, pp. 310-319.

S. Sakka, F. Ben Ayed, J. Bouaziz, (2012), Mechanical properties of tricalcium phosphate–alumina composites, *IOP Conf Series: Mat Sc Eng.*, Vol. 28, p. 012028.

S.S. Jensen, N. Broggini, E. Hjorting-Hansen, R. Schenk, D. Buser, (2006), Bone Healing and Graft Resorption of Autograft, Anorganic Bovine Bone and beta-Tricalcium Phosphate, a Histologic and Histomorphometric Study in the Mandibles of Minipigs, *Clin Oral Imp Res*., Vol. 17, pp. 237–243.

Yashima, A. Sakai, T. Kamiyama, A. Hoshikawa, (2003), Crystal Structure Analysis of β Tricalcium Phosphate $Ca_3(PO_4)_2$ by Neutron Powder Diffraction, *J Solid State Chem.*, Vol. 175, pp. 272−277.

Y.J. Horng, (1994), Fabrication and Mechanical Properties of Hydroxyapatite-Alumina Composites, *Mat Sc Eng C*, Vol. 2, pp. 77−81.